

## 1 Introduction

The development of three-dimensional (3D) multichip stacking technology has become essential to increase functionality and memory capacity in more complex architectures and smaller-form factor packages. Wafer thinning is required to reduce die thickness from original 750  $\mu\text{m}$  to 50  $\mu\text{m}$  or lower. Traditional dispense die-attach method with paste material is not capable of handling thinner dies. Wafer level films (WLFs) for die-to-die or die-to-substrate attachment were introduced in Refs. [1–6]. WLFs usually have a low glass transition temperature and substantially low Young's modulus (can be a few megapascals) at soldering reflow temperature. Figure 1 is a plot of storage modulus of a die-attach film with and without moisture [2,5]. It can be seen that the modulus decreases substantially when the temperature exceeds the glass transition temperature. As a consequence, film rupture may take place during the reflow process. Figure 2( ) is a through transmission scanning acoustic microscopy image of a  $6 \times 6$  array stacked-die chip scale package (CSP) panel, showing massive failures inside packages (black regions) after the reflow. A cross-

section view of a package confirms a large-scale cracking and voiding in the die-attach film attached to the substrate (called as the bottom layer film), as shown in Fig. 2( ). Other layers of films, which are sandwiched by dies, remain intact. Moisture is believed to be responsible for the failures. The bottom layer film absorbs moisture through the plastic substrate, while films in other layers absorb much less moisture. Therefore, no failures happen in other layers. It is noted that such a cohesive failure mode is different from the traditional interface delamination during the reflow, in which adhesion reduction due to moisture is the root cause [7–9].

Numerous designs of the experiment were executed for material screening and process optimization in developing stacked-die CSPs [2–5]. It has been found that package failure rates are very sensitive to substrate thickness and reflow profiles. Moisture uptake and transport during soldering reflow has been determined to be the root cause for these failures [2–5]. In the present study, the direct concentration approach (DCA) and the whole-field vapor pressure model developed in Part I of this work are applied to 3D ultrathin stacked-die CSPs. A simple bimaterial model, which represents a structure of the bottom layer film attached to a substrate, is analyzed first. Moisture redistribution, film “oversaturation,” and vapor pressure evolution during the reflow are studied in detail with this model. Two scenarios of vapor pressure buildup at reflow are identified. The DCA and whole-field vapor pressure

<sup>1</sup>Corresponding author.

Contributed by the Electrical and Electronic Packaging Division of ASME for publication in the JOURNAL OF ELECTRONIC PACKAGING. Manuscript received September 18, 2008; final manuscript received March 22, 2009; published online July 31, 2009. Assoc. Editor: Cemal Basaran.

analysis are then applied to ultrathin CSPs with different substrate

60°C/60% RH	Mat1	Mat2
Diffusivity $D$ (mm <sup>2</sup> /s)	$1.28 \times 10^{-5}$	$2.93 \times 10^{-5}$
$\rho_{sat}$ (kg/m <sup>3</sup> )	4.7	4.512
Solubility $S$ (kg/m <sup>3</sup> Pa)	$3.92 \times 10^{-4}$	$3.76 \times 10^{-4}$

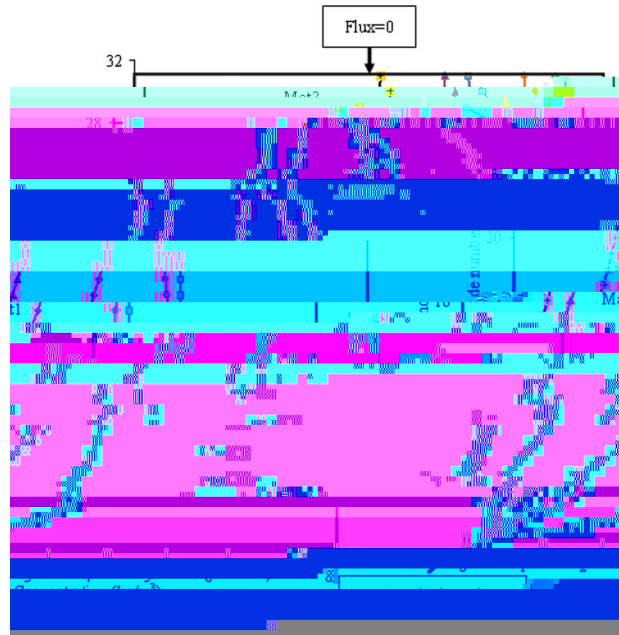
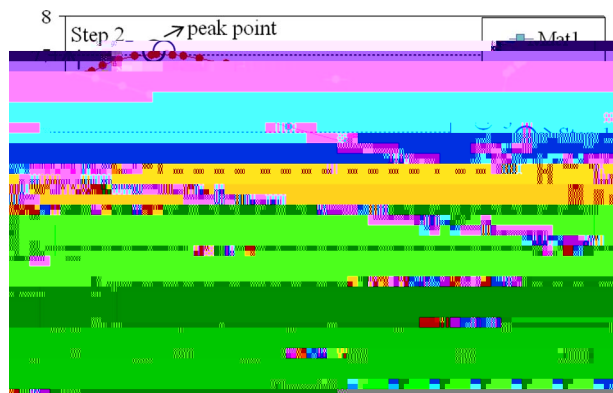
60°C/60% RH [11]. In the following, only the results in step 2 are shown (reflow process).

Figure 4 shows the results of moisture concentration in film and substrate at the interface as a function of time. It is observed that the moisture concentration in film has a “jump” in the beginning, while there is a drop in the substrate when desorption takes place. This is due to the new continuity requirement according to Eq. (1). It can be seen that the moisture concentration in film increases first, and then decreases with time. The local moisture gradient drives more moisture diffusing into the film in the beginning of the reflow process. Such a phenomenon is called oversaturation.

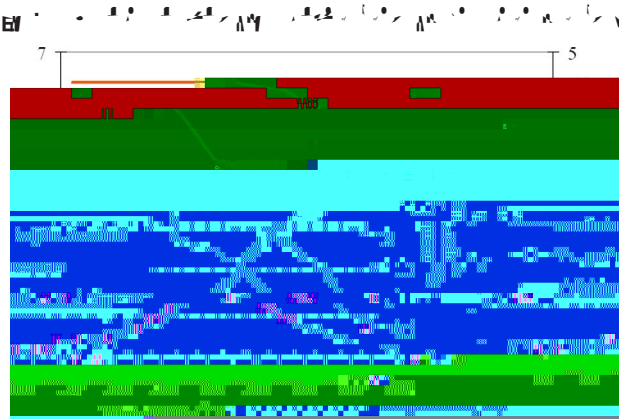
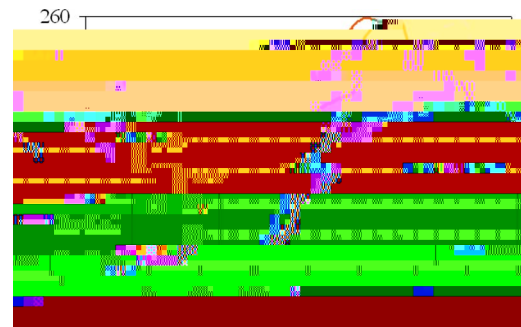
The distributions of moisture concentration in thickness direction at different times for Step 2 are plotted in Fig. 5. The moisture concentration at the boundary exterior is always zero. The moisture concentration is obviously discontinuous at the interface. In the beginning, the moisture concentration at the interface is redistributed according to the new continuity requirement. The redistribution causes moisture in the substrate at the interface less than in the bulk and moisture in the film at the interface greater than in the film bulk. Such a local moisture gradient will drive more moisture diffusing into the die-attach film from the substrate despite that an overall desorption process goes on. After a certain time (e.g., 20 s), moisture in the film eventually starts to decrease. It is noted that the total amount of moisture content at the interface, in the beginning, does not change much since the diffusion is not fast enough to change the total amount of moisture at the interface.

**3.2 Vapor Pressure Analysis.** In order to capture accurately the vapor pressure buildup during the reflow, a real reflow loading profile is applied here instead of using a step function in the preceding analysis. Figure 6 gives two reflow profiles that will be used in the subsequent analysis. Profile 1 in Fig. 6 is applied here. Several incremental steps are divided to simulate such an actual

200°C/60% RH	Mat1	Mat2
Diffusivity $D$ (mm <sup>2</sup> /s)	$4.72 \times 10^{-4}$	$6.43 \times 10^{-4}$
$\rho_{sat}$ (kg/m <sup>3</sup> )	4.7	9.024
Solubility $S$ (kg/m <sup>3</sup> Pa)	$5.05 \times 10^{-6}$	$9.7 \times 10^{-6}$



profile. The free volume fraction  $\phi$  is assumed to be 0.05 [11,12]. Figure 7 plots the vapor pressure and moisture concentration in the die-attach during the reflow. Results show that the vapor pressure increases exponentially and coincides with the saturated water vapor pressure curve. This implies that the moisture is in the mixed liquid/vapor state, according to Eq. (2). Around 220°C, the vapor pressure reaches a peak value (about 3 MPa) and then starts to decrease gradually even though the temperature continues to

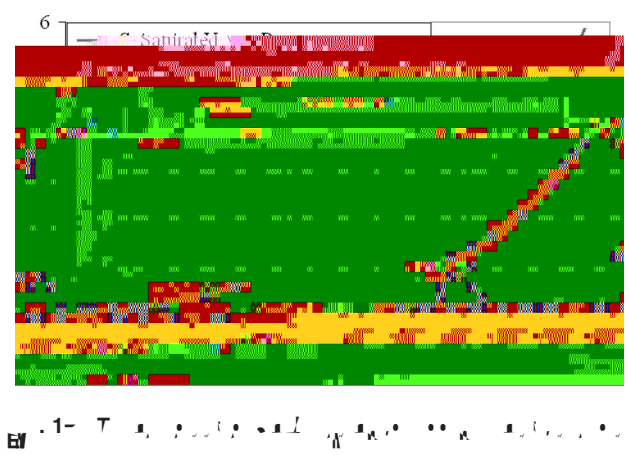
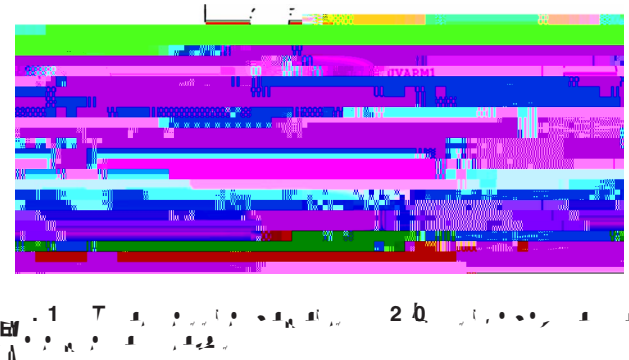
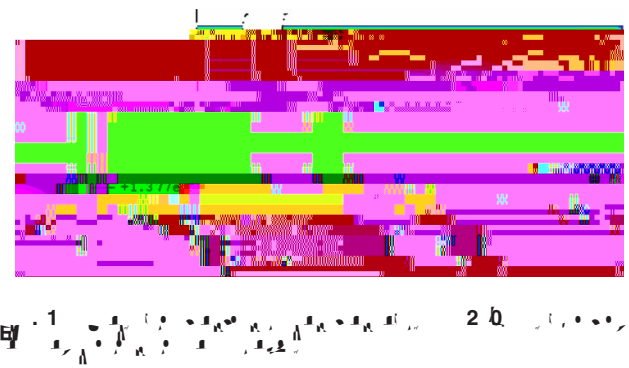
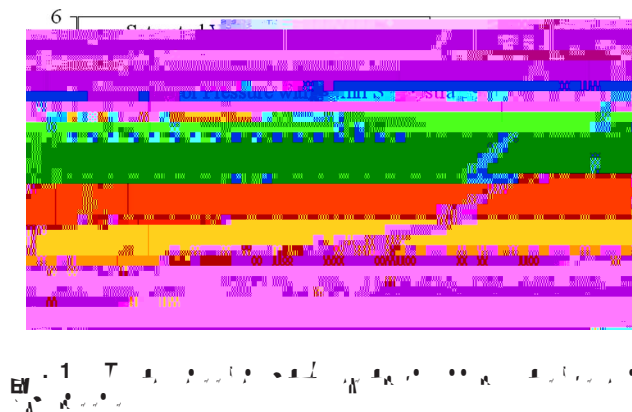
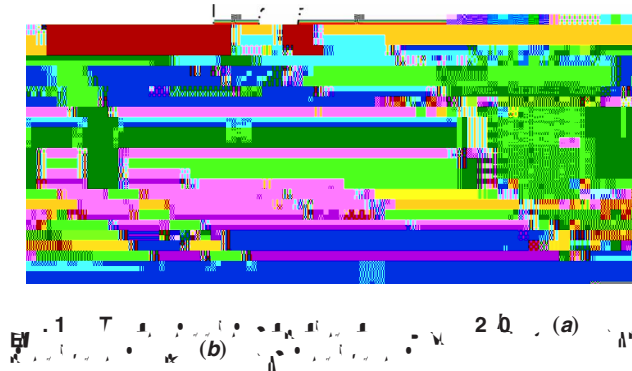
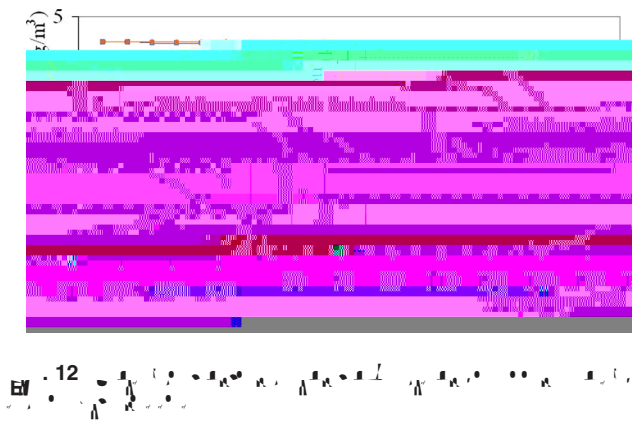


increase. This is because moisture diffuses out of the package during the reflow. When there is no sufficient residual moisture remaining in the film to keep it as a binary state, the vapor pressure will decrease.

Two scenarios of vapor pressure buildup during the reflow have been identified [2], as shown in Figs. 8 and 9, respectively. Before the reflow process starts, moisture condenses in nanopores or free volumes. With increasing temperature, more and more moisture will be vaporized. At the same time, the moisture concentration will decrease as more and more moisture will be diffused out of the package. At a certain point (temperature), the moisture may become fully vaporized. This point is a transition temperature for moisture from a binary state to a single vapor state. When the

the

Atpor



remains saturated at 260°C. Experimental results [4] showed that the failure rate for the thicker substrate is much higher for the thinner substrate, which are consistent with the DCA predictions.

**4.2 Effect of Reflow Profile.** Two different reflow profiles shown in Fig. 6 are applied here. These two profiles satisfy the JEDEC standard specification on temperature ramp up as a function of time. The main difference in these two profiles is that Profile 2 has an extended time period (approximately about 90 s) before the temperature ramps up rapidly to the peak temperature from a temperature of 150°C, compared to the Reflow Profile 1. Both profiles have the same peak temperature of 260°C.

The package, with a substrate thickness of 280 μm, is used here to study the effect of the reflow profile. Figure 15 plots the contours of moisture concentration at 250°C for these two reflows. When Reflow Profile 2 is applied, the moisture concentration in the bottom layer film is 34% less than with Reflow Profile 1. This is because Reflow Profile 2 has a longer exposure time at a level of temperature of 150°C to allow more moisture to be

released before it ramps up. Figure 16 plots the contours of vapor pressure at 250°C subjected to the two profiles, respectively. For Profile 2, the vapor pressure in the bottom layer film is 27% less than with Profile 1.

Figure 17 plots the vapor pressure evolution in the bottom layer film. It can be seen that the vapor pressure buildup under Profile 2 follows Scenario I with a vapor pressure drop at the temperature of 240°C, while the vapor pressure under Profile 1 follows Scenario II with a saturated water vapor pressure. These results are consistent with the experimental observations [5].

## 5 Discussions

In the preceding analysis, thermal stresses are not taken into considerations. Vapor pressure is presumed to be a dominant driving force for film rupture. Since the film modulus at the reflow temperature is extremely low (only a few megapascals), thermal stress is orders lower than the modulus. Even the finite-deformation theory is applied, the critical void volume fraction for the material to collapse is relatively small [15–17]. This implies that thermal stress is a small fraction of the peak vapor pressure.

Huang et al. [3] performed finite element analysis and showed that thermal stress is in a compressive state at the reflow since the film expansion is constrained by surrounding materials with relatively higher stiffness.

From the experimental data and vapor pressure analysis, the critical stress for film to rupture is in a very narrow range, say, between 2 MPa and 6 MPa (a very rough estimate). A finite single spherical void model was introduced previously by one of the authors [1,15,16]. When the hyperelastic model is applied for a rubbery material, a nonlinear and nonmonotonic relationship between vapor pressure and void volume fraction is obtained within the context of finite-deformation theory. This defines a critical stress for the occurrence of unstable void growth. The critical stress is found to be in the same order of Young's modulus of the film when initial void volume fraction is between 0.01 and 0.05 [15,16]. Although a single finite spherical void model is too simple, it shed light on the mechanism of unstable void growth within the context of finite-deformation. It is also observed that such a film failure is caused by a hydrostatic stress. Huang et al. [3] introduced Gent and Lindley's [17] solution for a single spherical void in an infinite medium to explain the cavitation in a rubbery material and concluded that the failure is modulated by the modulus and surface energy of the material, as well as the initial void size.

Cohesive film failures at the reflow have not been observed previously when the dispense die-attach assembly method is applied [7-9,18,19]. A die-attach paste material has a much higher modulus than a wafer-level die-attach film. A reasonable estimate of Young's modulus for a die-attach paste material is at least 100 MPa at the reflow temperature [1]. In this case, according to the analysis from a single void model, cohesive rupture is not a concern, rather it is an interfacial delamination. Most of the previous studies focused on the interfacial delamination [7-9,18,19]. Another unique characteristic, for the ultrathin CSP package, is moisture desorption during the reflow process. Moisture loss along the substrate/film interface becomes significant during the reflow. However, for a regular type package, significant moisture is lost only in the exterior of the package.

## 6 Conclusions

When above glass transition temperature, the saturated moisture concentration of the die-attach film increases. As a result, the film absorbs more moisture when the reflow process begins despite that an overall desorption goes on. This is referred to as oversatu-